

## Crystal structure of Cr-mullite

REINHARD X. FISCHER<sup>1,\*</sup> AND HARTMUT SCHNEIDER<sup>2</sup>

<sup>1</sup>Fachbereich Geowissenschaften der Universität, Klagenfurter Strasse, D-28359 Bremen, Germany

<sup>2</sup>Deutsches Zentrum für Luft- und Raumfahrt (DLR), Institut für Werkstoff-Forschung, D-51147 Köln, Germany

### ABSTRACT

A Rietveld refinement of Cr-doped mullite,  $\text{Cr}_{0.5}\text{Al}_{3.92}\text{Si}_{1.58}\text{O}_{9.79}$ , orthorhombic, space group *Pbam* [ $a = 7.56712(6)$  Å,  $b = 7.70909(6)$  Å,  $c = 2.90211(2)$  Å,  $V = 169.30$  Å<sup>3</sup>] revealed Cr to reside predominantly in the octahedrally coordinated M1 site. The mean M1-O distance of 1.935 Å is that expected from Al<sup>3+</sup> and Cr<sup>3+</sup> molar fractions obtained from the chemical analysis and structure refinement. The small displacement factors of the T\* and Oc\* sites indicate deficiencies in the electron densities which could be compensated by assuming additional Cr atoms. The predominant Cr incorporation into the M1 site causes an expansion of the octahedral bonds which is directly related to the observed lengthening of the *c* edge. The strong expansion of the long and elastic octahedral M1-Od bond in Cr-doped mullite, which would affect the *a* and *b* edges, is partly absorbed by a shortening of tetrahedral bonds.

### INTRODUCTION

Since the mineral mullite was first found in nature in the Isle of Mull in Scotland (Bowen and Greig 1924), it has been extensively studied due to its outstanding high-temperature properties. The composition of mullite refers to the general formula  $\text{Al}_2\text{Al}_{2-2x}\text{Si}_{2-2x}\text{O}_{10-x}$  where *x* denotes the number of oxygen vacancies. A range of  $\sim 0.20 < x < \sim 0.60$  is frequently described in literature (e.g., Cameron 1977). Recent studies prove that under special synthesis conditions this composition range can be extended to the  $\text{Al}_2\text{O}_3$ -rich site ( $x \leq 0.90$ , Fischer et al. 1996). The mullite structure consists of chains of edge-sharing  $\text{AlO}_6$  octahedra running parallel to the crystallographic *c* axis. The chains are crosslinked by  $(\text{Al},\text{Si})\text{O}_4$  tetrahedra forming double chains also running parallel to *c*. The thermodynamically stable modification of mullite with 60 mol%  $\text{Al}_2\text{O}_3$  (3  $\text{Al}_2\text{O}_3 \cdot 2 \text{SiO}_2$ , i.e., 3:2-mullite) is one of the most important ceramic phases with low thermal expansion, low thermal conductivity, excellent creep resistance, good chemical stability and high mechanical strength (Schneider et al. 1994).

Comprehensive work on Cr-doped mullites has been mainly done by spectroscopic methods. This material gained some interest due to its luminescent properties of Cr<sup>3+</sup> in glass ceramics to be used for laser technology (Andrews et al. 1986; Wojtowicz and Lempicki 1988). The site assignment of Cr in mullite is, however, still debated. Cr should be expected to prefer octahedral coordination, partly replacing Al<sup>3+</sup> at the M1 site. However, spectroscopic work done so far suggests that Cr is distributed over M1 and a more or less distorted interstitial position outside the  $\text{AlO}_6$  octahedron. Knutson et al. (1989) explain spectroscopic anomalies observed in Cr mullite by the disordered distribution of Cr, confirmed by Liu et al. (1990). Rager et al. (1990) interpreted their electron paramagnetic resonance-spectroscopic (EPR) data by Cr incorporation in the oc-

tahedral M1 site and in an interstitial octahedral site. This distribution of Cr over two octahedral sites has been confirmed by Ikeda et al. (1992) based on crystal-field spectroscopy. Also Nass et al. (1995) came to the same conclusion studying Cr-doped mullites by combined thermal analysis, quadrupole mass spectrometry, X-ray diffractometry, and electron microscopy. Piriou et al. (1996) and Bauchspies et al. (1996) stated that Cr occurs at both M1 and interstitial sites in  $\text{Cr}_2\text{O}_3$ -rich mullites. Rossouw and Miller (1999) investigated the same sample used here by incoherent channeling patterns (ICP) from characteristic X-ray emissions. They located Cr in the interstitial site at 0, 1/4, 0 which occurs at 1.93 Å from the next nearest M1 site, i.e., too close for simultaneous Al-Cr occupancy. It would imply that the M1 site is distorted, with vacancies equal to the number of Cr-atoms in the interstitial site which, however, was not detected. We discuss here the results of X-ray Rietveld refinements and give new and contrasting information on site preference in mullite.

### EXPERIMENTAL METHODS

#### Sample preparation

The starting material was 52 wt%  $\text{Al}_2\text{O}_3$  (VAW, 302), 38 wt%  $\text{SiO}_2$  (Ventron, 88316), and 10 wt%  $\text{Cr}_2\text{O}_3$ . The homogenized powder was pressed into pellets with 20 mm diameter and about 5 mm height. Calcination at 1650 °C for 10 days yielded mullite crystals up to 20 μm coexisting with a minor amount of silicate glass. The sample was treated with a HF/HCl acid mixture to dissolve the glass phase.

#### Chemical composition

Bulk chemical analysis performed by X-ray fluorescence analysis of the HF/HCl treated material yielded 61.9 wt%  $\text{Al}_2\text{O}_3$ , 27.8 wt%  $\text{SiO}_2$ , and 10.3 wt%  $\text{Cr}_2\text{O}_3$ . Microprobe analyses of various crystals in this sample gave weight fractions slightly deviating from the bulk chemical analysis: 60.0 wt%  $\text{Al}_2\text{O}_3$ ,

\*E-mail rfischer@min.uni-bremen.de

28.4 wt% SiO<sub>2</sub>, and 11.5 wt% Cr<sub>2</sub>O<sub>3</sub>. This discrepancy is due to the coexistence of two mullite compositions in this sample which was detected by high-resolution X-ray powder diffraction. Refinement of the lattice constants of the second component and the relation given by Fischer et al. (1996) indicate that there is no or only little Cr, the calculated composition being Al<sub>4.60</sub>Si<sub>1.40</sub>O<sub>9.70</sub>.

### X-ray data collection and Rietveld refinement procedure

X-ray data were collected on a Philips X'Pert diffractometer with a Ge monochromator in the primary beam yielding a strictly monochromatic radiation resulting in very sharp X-ray reflections. Details of data collection, crystallographic data, and definitions are given in Table 1. The background was fitted by a simple polynomial function. Intensities within eight times the full width at half maximum of a peak were considered to contribute to the central reflection. Peaks below  $2\theta = 50^\circ$  were corrected for asymmetry effects using Rietveld's (1969) algorithm. The pseudo-Voigt function was used for modeling the peak shape, with a refinable parameter defining the Lorentzian and Gaussian character of the peaks as a function of  $2\theta$ . Data were analyzed after Rietveld (1969) using a modified version of the PC-Rietveld plus package (Fischer et al. 1993). X-ray scattering factors in the proper valence states for Al, Si, and Cr were taken from the *International Tables for X-ray Crystallography* (Ibers and Hamilton 1974), that for O<sup>2-</sup> was taken from Hovestreydt (1983).

## RESULTS AND DISCUSSION

Shoulders in the low  $2\theta$  region and resolved peaks at higher angles in the high-resolution X-ray data clearly indicated the presence of two different mullite compositions (Fig. 1). This coexistence affects the accuracy of the lattice constant refine-

ments because of the overlapping reflections. The refinement of the lattice constants of the main component (Table 1) showed that it does not fit into the series of mullites with varying Si/Al in which a linear relation between the  $a$  edge and the molar alumina content is observed (Cameron 1977; Fischer et al. 1996). This is a clear indication of the Cr incorporation into this phase. We assumed that Cr occurs in the trivalent state only, as indicated by EPR studies (Rager et al. 1990), and that the Cr-doped mullite has the same average crystal structure as 3:2-mullite, with oxygen vacancies according to the general formula (Cr,Al)<sub>4+2x</sub>Si<sub>2-2x</sub>O<sub>10-x</sub> (where  $x$  denotes the number of oxygen vacancies per unit cell). The composition of the major component (> 80 wt%) in this sample is Cr<sub>0.50</sub>Al<sub>3.92</sub>Si<sub>1.58</sub>O<sub>9.79</sub>, corresponding to  $x = 0.21$ , somewhat lower than  $x = 0.25$  in 3:2-mullite. We calculated the starting site-populations for an initial model based on Al,Si-mullite according to Cameron (1977) and Fischer et al. (1994), yielding 2.0 Al atoms at M1,  $4 - 2x = 3.58$  atoms at T (2.0 Al and 1.58 Si),  $2x = 0.42$  (Al) atoms at T\*,  $2 - 3x = 1.36$  atoms at Oc, and  $2x = 0.42$  atoms at Oc\*. Atomic coordinates for the second component were taken from earlier work on mullites with similar composition (unpublished results) and kept fixed in the refinement. The refinement converged at  $R_{wp} = 12.8\%$  and  $R_B = 12.8\%$  showing a rather poor fit between observed and calculated intensities. Temperature factors were kept fixed as they refined to physically unrealistic values ( $> 7 \text{ \AA}^2$  for Oc\* and  $< 0$  for M1 and T\*) in an initial run. Difference Fourier analysis yielded the highest maximum ( $5 \text{ e/\AA}^3$ ) at 0, 0, 0, corresponding to the octahedral site. This could be interpreted as an indication for the presence of Cr which is a significantly stronger scatterer than Al. Albeit powder-diffraction data are usually less accurate than single-crystal data, this feature clearly contradicts the conclusion of Rossouw and Miller (1999) who ruled out the presence of significant Cr at M1. It also contrasts with spectroscopic work indicating high amounts of Cr in interstitial, distorted sites in Cr-rich mullites. To avoid a possible overestimation of the electron density at the special positions, a grid search analysis (Baur and Fischer 1986) was performed. A dummy Cr atom was shifted on a grid with step size 0.15 Å throughout the asymmetric unit. At each position, the occupancies were refined and recorded together with the respective residuals. As shown in the three-dimensional representation in Figure 2, there is a unique significant residual at the origin of the unit cell, confirming the Fourier results and the strong preference of Cr for the M1 site.

The occupancies of Cr and Al at M1 were then refined starting from the proportion of the chemical analysis (0.25 Cr + 0.75 Al) under constraint of full-occupancy of two atoms per formula unit (pfu). The refinement yielded 1.44 Al and 0.56 Cr pfu, which is very close to the results of the microprobe analysis. These results should correspond to an expansion of the octahedron due to Cr incorporation, and the observed mean M1-O bond should be related to the weighted averages of the ionic radii of <sup>63</sup>Cr and <sup>63</sup>Al, 0.615 and 0.535 Å, respectively (Shannon 1976). The mean M1-O distance calculated from the 10 mullite structures from Ban and Okada (1992) and Angel and Prewitt (1986) is 1.913 Å, and that calculated for 0.28 Cr + 0.72 Al is 1.935 Å, exactly the value obtained from Rietveld

**TABLE 1.** Experimental conditions and selected crystallographic refinement parameters

Philips X'Pert			
Radiation type, source	X-ray, CuK $\alpha_1$		
Discriminator	primary beam, germanium monochromator		
Divergence slit	0.25°		
Receiving slit	0.2 mm		
Data collection temperature	room temperature		
$2\theta$ range	15–150°		
Step size	0.02°		
Counting time per step	100 s		
Space group	<i>Pbam</i>		
<i>Z</i>	1		
Lattice parameters (Å)		Phase I	Phase II
	<i>a</i>	7.56712(6)	7.5584(4)
	<i>b</i>	7.70909(6)	7.7000(4)
	<i>c</i>	2.90211(2)	2.8915(1)
Standardless quantitative analysis		82.4 wt%	17.6 wt%
$R_{wp} = \sqrt{\frac{\sum_i (y_{io} - C \cdot y_{ic})^2}{\sum_i w_i y_{io}^2}}$		10.1%	
$R_B = \frac{\sum_k  I_{ko} - C \cdot I_{kc} }{\sum_k I_{ko}}$		5.2%	

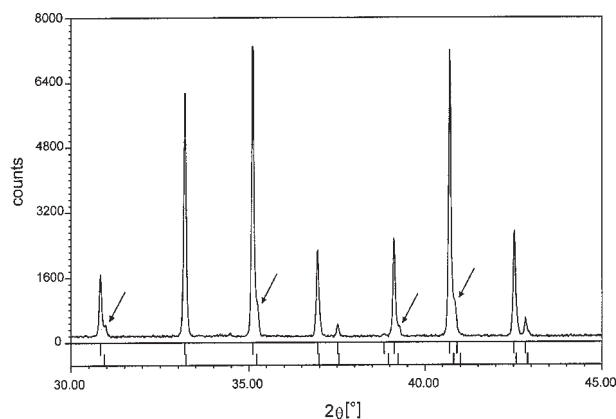


**FIGURE 1.** A section of the observed powder pattern between  $2\theta$  of 30 and  $45^\circ$ , showing the occurrence of two mullite phases. Arrows point to the peaks of the second phase. **(Top)** XRD spectrum. **(Bottom)** Line positions for the two phases are shown as two series of dashes.

refinement.

Crystal field, extended X-ray absorption fine structure (EXAFS), and especially time-resolved fluorescence spectra of  $\text{Cr}_2\text{O}_3$ -doped mullite have to be interpreted in terms of Cr incorporation into different structural sites (Ikeda et al. 1992; Bauchspiess et al. 1996; Piriou et al. 1996). The high field  $\text{Cr}^{3+}$  site in fluorescence spectroscopy corresponds to the M1 site while the low or intermediate field may be associated with a different incorporation mode of  $\text{Cr}^{3+}$ . Possible sites are the relatively wide channels running along the  $c$  edge, or sites close to the Oc oxygen vacancies. The refined atomic parameters show that T\* has an unusually low displacement factor of  $0.1 \text{ \AA}^2$  which could indicate that the scattering power of this site has been underestimated. Similar effects, less pronounced though, are observed for the Oc\* site. Refinement of T\* with a mixed Al/Cr occupancy (sum of Al + Cr constrained to 0.43 atoms pfu) yielded 0.39(1) Al and 0.04(1) Cr atoms with a B-value of  $0.5(3) \text{ \AA}^2$ . The  $R$  indices were not significantly affected. The latter model may only give some clues for additional Cr sites which could explain two different Cr sites detected by spectroscopy. The final refinement yielding the atomic parameters given in Table 2 is that obtained with Cr at the M1 site, and the final fit between observed and calculated powder patterns is shown in Figure 3. Refinement of small fractions of Cr in disordered interstitial sites is definitely beyond the resolution of a Rietveld refinement.

The discrepancy between the results from the Rietveld refinements and the spectroscopic data could be explained by

**TABLE 2.** Positional parameters, and isotropic displacement factors ( $\text{\AA}^2$ ), for Cr-doped mullite

Atom	$x$	$y$	$z$	$B$	Population
M1	0	0	0	0.52(3)	1.5 Al + 0.5 Cr
T	0.1482(2)	0.3416(2)	$\frac{1}{2}$	0.69(3)	2.00 Al + 1.57 Si
T*	0.2599(15)	0.2002(14)	$\frac{1}{2}$	0.1(2)	0.43 Al
Oab	0.3565(3)	0.4217(3)	$\frac{1}{2}$	1.31(7)	4 O
Oc	$\frac{1}{2}$	0	$\frac{1}{2}$	1.6(2)	2 O
Oc*	0.4360(33)	0.0479(32)	$\frac{1}{2}$	0.7(5)	0.43 O
Od	0.1275(3)	0.2249(3)	0	1.26(6)	4 O

Note: The site populations are calculated from microprobe analyses.

comparison with electron paramagnetic resonance (EPR) spectra. Cr-doped mullites give two sharp EPR signals near  $g_{\text{eff}} = 5$ , and a broad signal near  $g_{\text{eff}} = 2.2$ . The former was assigned to  $\text{Cr}^{3+}$  on the slightly distorted octahedral M1 site, whereas the latter was interpreted as coupling between neighboring magnetic moments due to the occurrence of  $\text{Cr}^{3+}$ - $\text{Cr}^{3+}$  clusters (Rager et al. 1990). These  $\text{Cr}^{3+}$ - $\text{Cr}^{3+}$  interactions may be interpreted by the incorporation of  $\text{Cr}^{3+}$  solely into the octahedral M1 site, with a strong tendency to form  $\text{CrO}_6$  clusters along the octahedral chains running parallel to the  $c$  edge. According to this model, it is possible to distinguish between "internal"  $\text{CrO}_6$  octahedra with  $\text{Cr}^{3+}$  as next-nearest neighbors and "external"  $\text{CrO}_6$  octahedra with  $\text{Cr}^{3+}$  and  $\text{Al}^{3+}$  as next-nearest neighbors. The two types of  $\text{CrO}_6$  octahedra are likely to have slightly different distortions, which may explain the different  $\text{Cr}^{3+}$  signals in spectroscopic analysis.

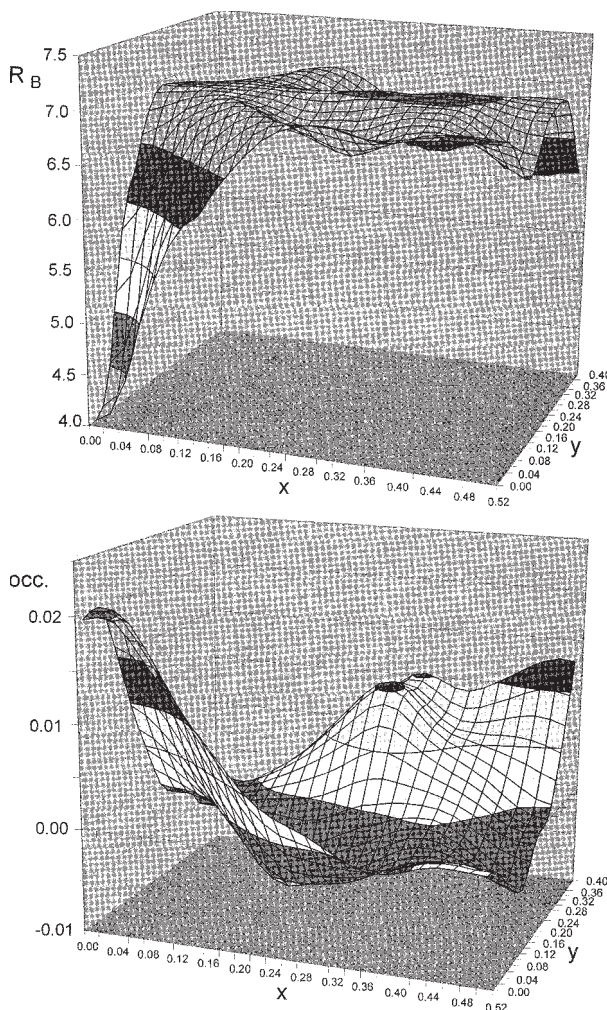


**FIGURE 2.** Three-dimensional representation of the grid-search analysis in the (001) plane with  $z = 0$ . **(Top)**  $R_B$  values from refinements of a hypothetical Cr atom in  $x, y, 0$  plotted for all positions in  $x$  from 0.00 to 0.52 and  $y$  from 0.00 to 0.40 in steps of 0.02. **(Bottom)** Refined populations (number of atoms pfu =  $\text{Occ} \cdot 8$ ) of Cr corresponding to the refinement steps in the top figure.

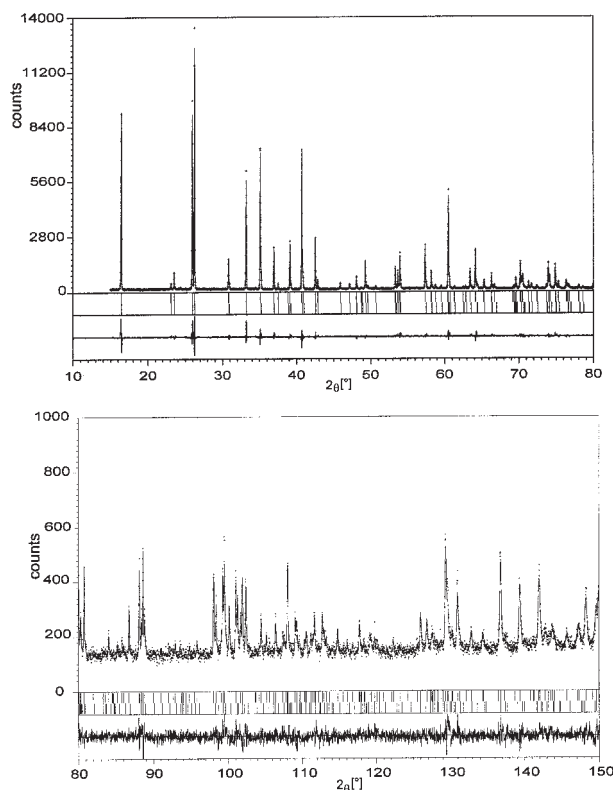


FIGURE 3. Observed (crosses) and calculated (solid line) powder patterns with difference curves underneath. Peak positions permitted by the cell metric are indicated by tick marks (first row: Cr-doped mullite, second row: additional mullite phase).

Our results still contradict the observations from the ALCHEMI (atom location by channeling enhanced microscopy) studies recently done by Rossouw and Miller (1999). These authors concluded that in Cr-rich mullite nearly all or all  $\text{Cr}^{3+}$  enters the interstitial site at  $0, 1/4, 0$ . However, Cr-incorporation at  $0, 1/4, 0$  is crystallochemically questionable as its distance to the next-nearest M1 site is extremely short ( $1.93 \text{ \AA}$ ). Because there is no indication for vacancies at M1, this would lead to an unacceptable repulsion between Cr and Al. If the coordinates are refined in Wyckoff position  $4g (x,y,0)$ , starting with  $0, 0.25, 0$ , the Cr atom is shifted far away from this position, yielding a very high temperature factor and residuals of  $R_{wp} = 18.7\%$  and  $R_B = 17.4\%$ . Actually, Rossouw and Miller (1999) referred to a Rietveld refinement of the same sample done in their laboratories that yielded results similar to ours. They concluded that the Rietveld refinements are less suitable in this case as they represent the average structure, and that the ICP results unambiguously indicate that Cr resides at the well-defined interstitial site I. The need for cation vacancy in the M1 site at  $1.93 \text{ \AA}$  from site I has been neither investigated nor discussed by Rossouw and Miller (1999). On the contrary, their results are based on the same formula unit as derived in our work, with  $x = 0.212$  oxygen vacancies and a fully occupied M1 position.

Selected interatomic distances are listed in Table 3. Mean T-O and T\*-O distances agree well with previously described

structures of mullites whereas the mean M1-O is considerably larger than usually observed except for the high alumina mullite. Among the individual distances, major changes are observed for M1-Od ( $1.984 \text{ \AA} \times 2$ ) which defines the octahedral cross section in the (001) plane. It is less pronounced for the M1-Oab distances ( $1.910 \text{ \AA} \times 4$ ) which represents the octahedral plane perpendicular to the (001) plane. The M1-Od distances are 1.7%, and the M1-Oab distances 0.8% longer than in a 3:2 mullite reference structure (sample SP1400.1 after Ban and Okada 1992). Because the octahedral axes in the (001) plane are tilted by about  $29^\circ$  from the crystal axes, changes in M1-Od are not linearly related to the changes in the cell constants, whereas the enlargement in  $c$  directly reflects that of the M1-Oab distance. The relation between  $c$  and  $\langle \text{M1-O} \rangle$  is given by  $c = 2 \times \sin[\angle (\text{Oab-M1-Oab})/2] \times \langle \text{M1-O} \rangle$ , with the angle  $(\angle \text{Oab-M1-Oab}) = 98.9^\circ$  in the plane perpendicular to (001). The lengthening of the bonds affects the  $a$  and  $b$  edges as well, and  $a$  is about 0.3%, and  $b$  about 0.2% longer than in the 3:2 mullite reference structure. Considering that the incorporation

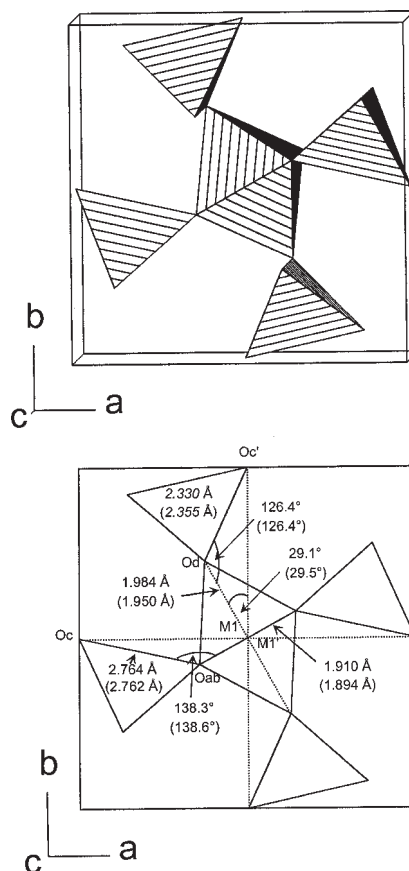


FIGURE 4. The crystal structure of Cr-doped mullite. (a) The  $\text{M1O}_6$  octahedron with four neighboring  $\text{TO}_4$  tetrahedra. Projection parallel to  $c$  and rotated by  $5^\circ$  about  $a$  and  $b$ . (b) The same view as in  $a$ , without the rotation. Numbers refer to distances and angles in Cr-doped mullite (top) and in a 3:2 mullite reference structure (Ban and Okada 1992; in parentheses). Values in italics represent distances projected onto the (001) plane.  $\text{Oc}'$  is the projection of  $\text{Oc}$  at  $z = 0$ , and  $\text{M1}'$  the projection of  $\text{M1}$  at  $z = 1/2$ .

**TABLE 3.** Selected interatomic distances (Å) for Cr-doped mullite

M1 – Oab ×4	1.910(2)	T – Oc	1.658(2)	T* – Od ×2	1.773(7)
M1 – Od ×4	1.984(2)	T – Oab	1.693(3)	T* – Oc*	1.776(27)
		T – Od ×2	1.714(2)	T* – Oab	1.857(11)
mean	1.935	mean	1.695	mean	1.795

of Cr into the M1 site affects mainly the M1-Od bond, we would expect that the influence on  $b$  is greater than on  $a$ , but the reverse is actually observed. Figure 4 shows the mullite structure, with the M1 octahedron and the four adjacent  $TO_4$  tetrahedra. The  $a$ -edge is defined in the triangle M1'-Oab-Oc (M1' is the projection of M1 on the octahedral edge in  $z = 1/2$ ) where M1'-Oc represents  $1/2 \times a$ . Since the angle about Oab and the tetrahedral edge do not differ much from the 3:2 reference structure, the lengthening of  $a$  mainly reflects the expansion of the M1-Oab bond. The  $b$ -edge can be calculated from the geometric arrangement in the triangle M1-Od-Oc'. However, the expansion of the M1-Od bond is compensated by a shortening of the tetrahedral edge from 2.761 Å in the reference structure to 2.745 Å in the Cr-doped mullite; their projections onto the (001) plane are 2.355 Å and 2.330 Å, respectively (Fig. 4).

#### ACKNOWLEDGMENT

We thank R. Oberti and A. Gualtieri for their careful reviews and suggestions.

#### REFERENCES CITED

- Andrews, L.J., Beall, G.H., and Lempicki, A. (1986) Luminescence of  $Cr^{3+}$  in mullite transparent glass ceramics. *Journal of Luminescence*, 36, 65–74.
- Angel, R.J. and Prewitt, C.T. (1986) Crystal structure of mullite: A re-examination of the average structure. *American Mineralogist*, 71, 1476–1482.
- Ban, T. and Okada, K. (1992) Structure refinement of mullite by the Rietveld method and a new method for estimation of chemical composition. *Journal of the American Ceramic Society*, 75, 227–230.
- Bauchspiess, K.R., Schneider, H., and Kulikov, A. (1996) EXAFS studies of Cr-doped mullite. *Journal of the European Ceramic Society*, 16, 203–209.
- Baur, W.H. and Fischer, R.X. (1986) Recognition and treatment of background problems in neutron powder diffraction refinements. In Barrett, C.S., Cohen, J.B., Faber, J., Jenkins, R., Leyden, D.E., Russ, J.C., and Predecki, P.K., Eds., *Advances in X-ray analysis* Vol. 29, p. 131–142. Plenum Press, New York and London.
- Bowen, N.L. and Greig, J.W. (1924) The system  $Al_2O_3$ - $SiO_2$ . *Journal of the American Ceramic Society*, 7, 238–254.
- Cameron, W.E. (1977) Mullite: A substituted alumina. *American Mineralogist*, 62, 747–755.
- Fischer, R.X. (1993) Divergence slit corrections for Bragg Brentano diffractometers. *European Powder Diffraction Conference EPDIC 3* (Vienna). Abstracts, 25.
- Fischer, R.X., Lengauer, C., Tillmanns, E., Ensink, R.J., Reiss, C.A., and Fanter, E.J. (1993) PC-Rietveld plus, a comprehensive Rietveld analysis package for PC. *Materials Science Forum*, 133–136, 287–292.
- Fischer, R.X., Schneider, H., and Schmücker, M. (1994) Crystal structure of Al-rich mullite. *American Mineralogist*, 79, 983–990.
- Fischer, R.X., Schneider, H., and Voll, D. (1996) Formation of aluminum rich 9:1 mullite and its transformation to low alumina mullite upon heating. *Journal of the European Ceramic Society*, 16, 109–113.
- Hovestreydt, E. (1983) On the atomic scattering factor for  $O^{2-}$ . *Acta Crystallographica*, A39, 268–269.
- Ibers, J.A. and Hamilton, W.C., Eds. (1974) *International tables for X-ray crystallography*, vol. 4, p. 99–149. Kynoch, Birmingham, U.K.
- Ikeda, K., Schneider, H., Akasaka, M., and Rager, H. (1992) Crystal-field spectroscopic study of Cr-doped mullite. *American Mineralogist*, 77, 251–257.
- Knutson, R., Liu, H., Yen, W.M., and Morgan, T.V. (1989) Spectroscopy of disordered low-field sites in  $Cr^{3+}$ : Mullite glass ceramic. *Physical Reviews B*, 40, 4264–4270.
- Liu, H., Knutson, R., Jia, W., Strauss, E., and Yen, W.M. (1990) Spectroscopic determination of the distribution of  $Cr^{3+}$  sites in mullite ceramics. *Physical Reviews B*, 41, 12888–12894.
- Nass, R., Tkalcec, E., and Ivankovic, H. (1995) Single phase mullite gels doped with chromium. *Journal of the American Ceramic Society*, 78, 3097–3106.
- Priou, B., Rager, H., and Schneider, H. (1996) Time-resolved fluorescence spectroscopy of  $Cr^{3+}$  in mullite. *Journal of the European Ceramic Society*, 16, 195–201.
- Rager, H., Schneider, H., and Graetsch, H. (1990) Chromium incorporation in mullite. *American Mineralogist*, 75, 392–397.
- Rietveld, H.M. (1969) A profile refinement method for nuclear and magnetic structures. *Journal of Applied Crystallography*, 2, 65–71.
- Rossouw, C.J. and Miller, P.R. (1999) Location of interstitial Cr in mullite by incoherent channeling patterns from characteristic X-ray emission. *American Mineralogist*, 84, 965–969.
- Schneider, H., Okada, K., and Pask, J.A. (1994) *Mullite and mullite ceramics*, 201 p. Wiley, Chichester, U.K.
- Shannon, R.D. (1976) Revised effective ionic radii and systematic studies of interatomic distances in halides and chalcogenides. *Acta Crystallographica*, A32, 751–767.
- Wojtowicz, A.J. and Lempicki, A. (1988) Luminescence of  $Cr^{3+}$  in mullite transparent glass ceramics (II). *Journal of Luminescence*, 39, 189–203.

MANUSCRIPT RECEIVED JUNE 1, 1999

MANUSCRIPT ACCEPTED APRIL 3, 2000

PAPER HANDLED BY ROBERTA OBERTI